THE JOURNAL OF PHYSICAL CHEMISTRY B

ARTICLE

pubs.acs.org/JPCB

Understanding Liquid Mixture Phase Miscibility via Pair Energy Parameter Behaviors with Respect to Temperatures Determined from Molecular Simulations

Suk Yung Oh and Young Chan Bae*

Division of Chemical Engineering and Molecular Thermodynamics Laboratory, Hanyang University, Seoul 133-791, Korea

ABSTRACT: The miscibility behaviors of binary liquid mixtures were studied by a combination of molecular simulations and thermodynamic theories. Pairwise interaction parameters were obtained from molecular simulations that accounted for the effect of temperature. From a thermodynamic perspective, different types of liquid−liquid equilibrium (LLE) and different degrees of miscibility can be expressed in terms of energy behaviors with respect to temperature. Our simulation results proved this viewpoint by showing a correspondence between the simulation results and experimental observations. To describe phase diagrams, thermodynamic modeling is presented using the energy parameters obtained from the simulations. Correlations are needed to correct size mismatches between the simulations and the thermodynamic model. Using this method, not only the upper critical solution temperature (UCST) but also the closed-loop miscibility phase diagrams could be calculated without requiring additional parameters for specific interactions. The utility of this method is demonstrated for mixtures containing water, hydrocarbon, alcohols, aldehydes, ketones, chlorides, amines, nitriles, sulfides, and other organic liquids in various temperature ranges. The method presented in this paper can facilitate the understanding of the miscibilities in binary liquid mixtures from the viewpoint of thermal energy behaviors.

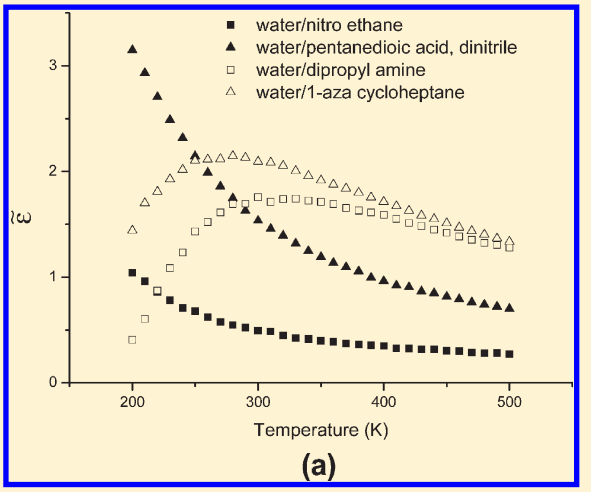

1. INTRODUCTION

Understanding the phase separation or miscibility behaviors of fluid mixtures is one of the cornerstones of chemical engineering. The design of separation processes such as distillation, absorption, and extraction requires quantitative estimates of the phase equilibrium properties of fluid mixtures. Knowledge of the miscibility properties of specific systems is often necessary to design separation processes or to predict process performance.

Miscibility behavior can be illustrated by calculating the free energy of mixing as a function of composition at different temperatures. The Flory−Huggins (FH) lattice model[1,2] is the most widely used theory to judge miscibility or derive phase diagrams. The FH model illustrates the competition between the entropy of mixing and the attractive forces that produce phase separation in a simple way. Although some refinements to the FH model have been made,[3,4] the lattice cluster theory[5−8] (LCT) was a landmark because it is a formal exact mathematical solution of the FH lattice with a complete and systematic analysis. However, its complexity of expression restricts its practical use and discrepancies exist when its results are compared to simulation results. To overcome these limitations, an advanced method of model development has been proposed that uses simulation results directly. For example, Hu et al.[9] simplified the LCT and determined universal parameters by comparison with Monte Carlo simulation results. A similar procedure was adopted by Oh et al.[10] for the development of the modified double lattice (MDL) model. These two models obtain accurate results while maintaining model simplicity.

Besides the lattice theory, other liquid state models are also extensively used in the calculation of the various properties of liquid mixtures. Schweizer and Curro[11,12] developed the systematic, continuum analytic approach to the equilibrium structure of molecular fluids based on their "polymer reference interaction site model" (PRISM) approach and the wide applications are reported[13,14] for phase behavior of various polymer systems. Lipson et al.[15−17] also used the continuum integral equation and its lattice contribution to analyze phase equilibrium and obtain thermodynamic properties. Recently, Curro, Grest, and co-workers[18−20] performed molecular dynamics simulations of polymers and the comparison study with PRISM theory. Guenza et al.[21,22] presented multiscale simulations and a coarse-grained model for polymeric liquid states.

Given some experimental data for limited conditions, thermodynamics provides procedures for generating data under other conditions. However, in many cases in which experimental information is not available, the ability to predict phase miscibility is

Received: January 6, 2011
Revised: March 15, 2011
Published: April 14, 2011

restricted. Failure to achieve this goal follows from inadequate understanding of liquid structures and intermolecular forces.

Molecular simulations along with the use of appropriate force fields may help solve these problems. Because of the ever-increasing power of computers, in recent years impressive advances have been made in simulating the properties of fluids and their mixtures. In the past decade, many scientific papers have reported using combinations of the thermodynamic model and molecular simulations.[23−27] Unfortunately, most of these studies included only a few cases so that the universality is insufficient and had limitations of describing a complete phase diagram.

In this work, we performed molecular simulations of various types of binary liquid mixtures using the COMPASS (condensed-phase optimized molecular potentials for atomic simulation studies) force field method.[28,29] Interaction energy parameters were obtained at different temperatures, and using these results, relative miscibilities were compared in a qualitative manner. All of the simulation results in this study are divided into two types of energy behavior. The liquid−liquid equilibrium (LLE) types of each mixture, including an upper critical solution temperature (UCST), a lower critical solution temperature (LCST), and a closed-loop miscibility (having both a UCST and a LCST) were predicted depending on the type of energy behavior. Finally, we presented a correlation method connecting the simulation results into a thermodynamic model to describe the temperature−composition phase diagrams. A scaling concept was introduced to correct size mismatches between the simulations and the thermodynamic model. MDL theory was adopted for the thermodynamic model, and the calculated results were compared with experimental data.

2. SIMULATION DETAILS

The systems investigated in the simulations were binary liquid mixtures of small molecules chosen from the LLE data collection.[30] Pairwise interaction energy values were computed using a molecular simulation technique developed by Blanco et al.,[23,31] available in the Blends module of the commercial software Materials Studio (version 4.4) from Accelrys. The structures of the molecules were first constructed and the geometries were then optimized by energy minimization. Many configurations of the two molecules were generated and the pair interaction energy was calculated. In this way, the Monte Carlo method was used for both generating thousands of different orientations and calculating the corresponding pair interaction energy. Finally, pairwise interaction energy values (ε_{11}, ε_{22}, and ε_{12}) were determined by averaging all accepted configurations.

The COMPASS force field was used in these simulations, as it has been specially optimized to provide accurate cohesive properties for molecules containing a wide range of functional groups.[28,29] The potential energy of a system can be expressed as a sum of the valence (or bond), cross term, and nonbond interactions:

$$E_{\text{total}} = E_{\text{valence}} + E_{\text{cross}} + E_{\text{nonbond}} \quad (1)$$

where the valence term represents the internal coordinates of bond, angle, torsion angle, and out-of-plane angle, and the cross term includes combinations of two or three internal coordinates. The cross term is important for predicting the vibration frequencies and structural variations associated with conformational changes. The nonbond interactions, which include the van der Waals term, an electrostatic interaction, and hydrogen-bonding interactions, are used for interactions between pairs of atoms that are separated by two or more intervening atoms or those that belong to different molecules.

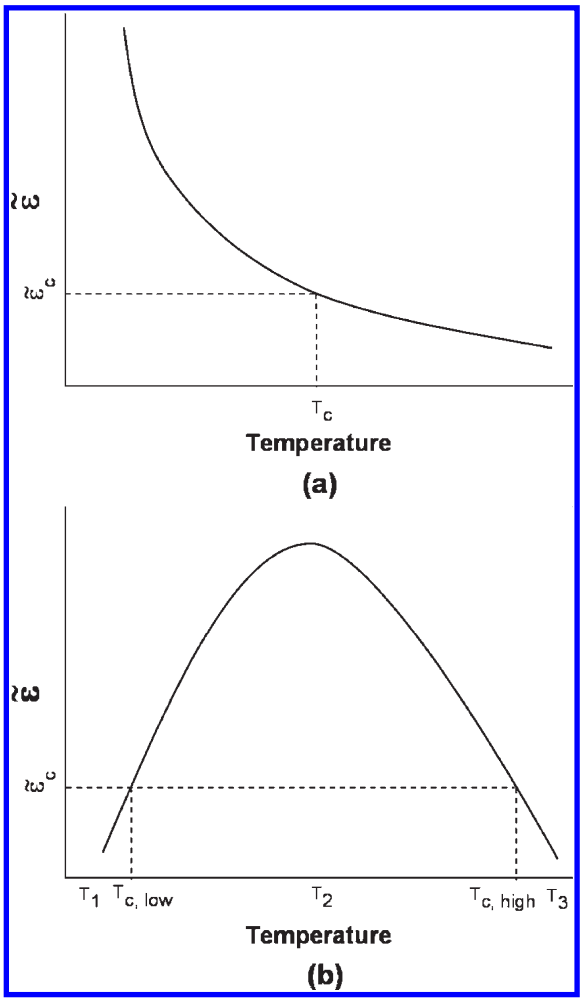

Figure 1. Schematic representations of contributions to reduced interchange energy parameters: (a) type A energy behavior; (b) type B energy behavior.

All simulations were carried out in the temperature range between 200 and 500 K at intervals of 10 K. We set the number of energy samples at 10^7, the cluster samples at 10^4, and the iterations per cluster at 20.

3. THERMODYNAMICS

3.1. Thermodynamic Models. The FH theory is based on a lattice model wherein all lattice sites are occupied by segments of molecules. A mean-field approximation was used to obtain the Helmholtz energy of mixing, ΔA. In the mean-field approximation, ΔA is the sum of a combinatorial entropy and a simple term for the energy of mixing[1,2]

$$\frac{\Delta A}{N_r kT} = \frac{\phi_1}{r_1}\ln\phi_1 + \frac{\phi_2}{r_2}\ln\phi_2 + \chi\phi_1\phi_2 \quad (2)$$

where N_r is the total number of lattice sites, r_i is the number of lattice sites occupied by a molecule of component i, ϕ_i is the

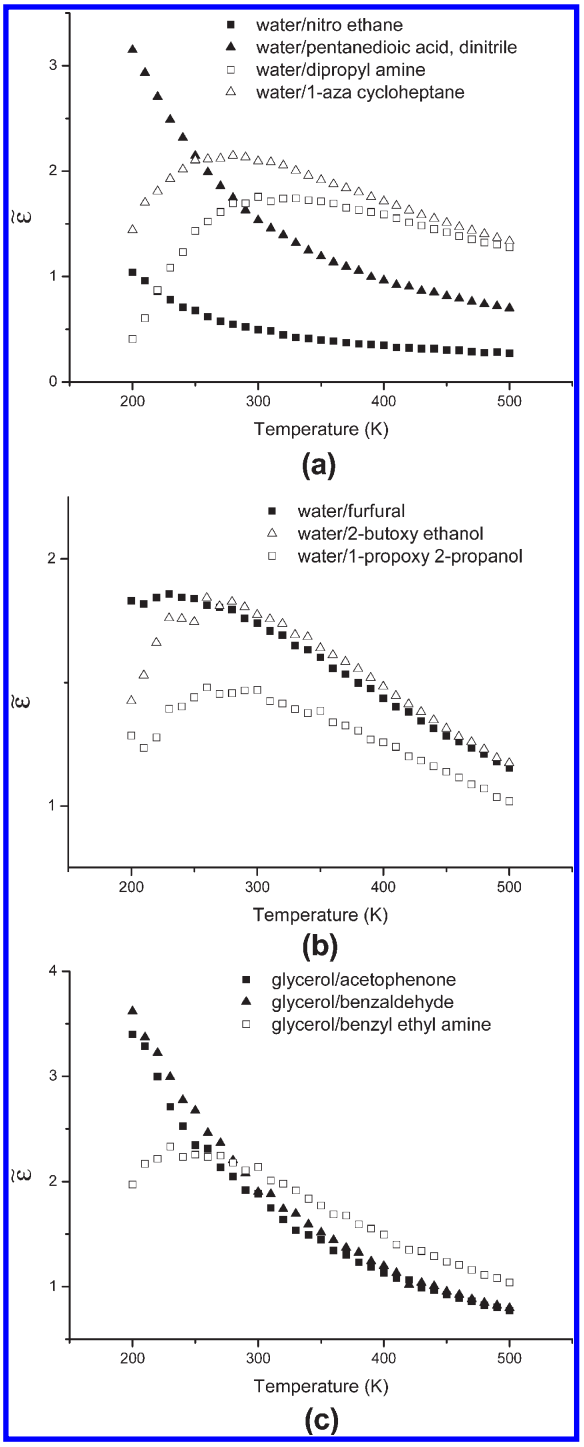

Figure 2. Simulation results: (a) water/nitrogen compounds; (b) water/oxygen compounds; (c) glycerol mixtures.

volume fraction of component i, and kT has the usual meaning. The interaction parameter χ reflects nearest-neighbor interaction energies defined as

$$\chi = z\tilde{\varepsilon} \tag{3}$$

where z is the coordination number, the value of which for the cubic lattice model was taken as 6, and $\tilde{\varepsilon}$ is the reduced interchange energy, given by

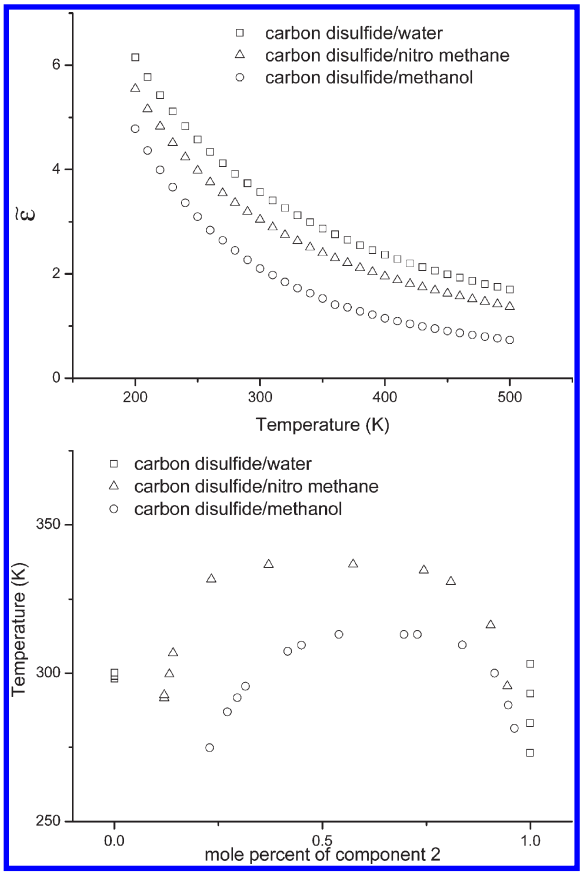

Figure 3. Simulation results and experimental data[30] for carbon disulfide mixtures.

$$\tilde{\varepsilon} = \varepsilon/kT = (\varepsilon_{11} + \varepsilon_{22} - 2\varepsilon_{12})/kT \tag{4}$$

where ε is the interchange energy between components 1 and 2, and ε_{ij} is the interaction energy of the $i-j$ pair. A variety of lattice models has been developed during the last half century; most are revised forms of the classical work of Flory and Huggins. MDL is one of the widely used lattice models,[10,32] which is defined as a form of the FH theory

$$\frac{\Delta A}{N_r kT} = \frac{\phi_1}{r_1}\ln\phi_1 + \frac{\phi_2}{r_2}\ln\phi_2 + \chi_{OB}\phi_1\phi_2 \tag{5}$$

where χ_{OB} is defined as

$$\chi_{OB} = C_\beta\left(\frac{1}{r_2} - \frac{1}{r_1}\right)^2 + \left(2 + \frac{1}{r_2}\right)\tilde{\varepsilon} - \left(\frac{1}{r_2} - \frac{1}{r_1} + C_\gamma\tilde{\varepsilon}\right)\tilde{\varepsilon}\phi_2 + C_\gamma\tilde{\varepsilon}2{\phi_2}^2 \tag{6}$$

where C_β and C_γ are universal constants with the values 0.1415 and 1.7986, respectively. These constants are determined by correlations with the Monte Carlo simulation results of Madden et al.[33]

We require the chemical potentials of components 1 and 2 to calculate the binary coexistence curve. They are given by

$$\frac{\Delta\mu_1}{kT} = \left[\frac{\partial(\Delta A/N_r kT)}{\partial N_1}\right]_{T,V,N_2} \tag{7}$$

dx.doi.org/10.1021/jp2001628 |J. Phys. Chem. B 2011, 115, 6051–6060

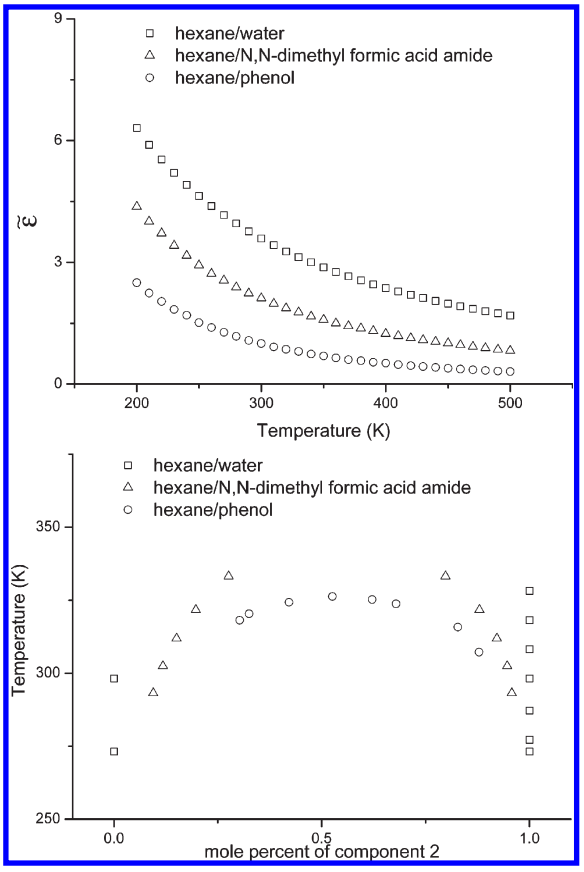

Figure 4. Simulation results and experimental data[30] for hexane mixtures.

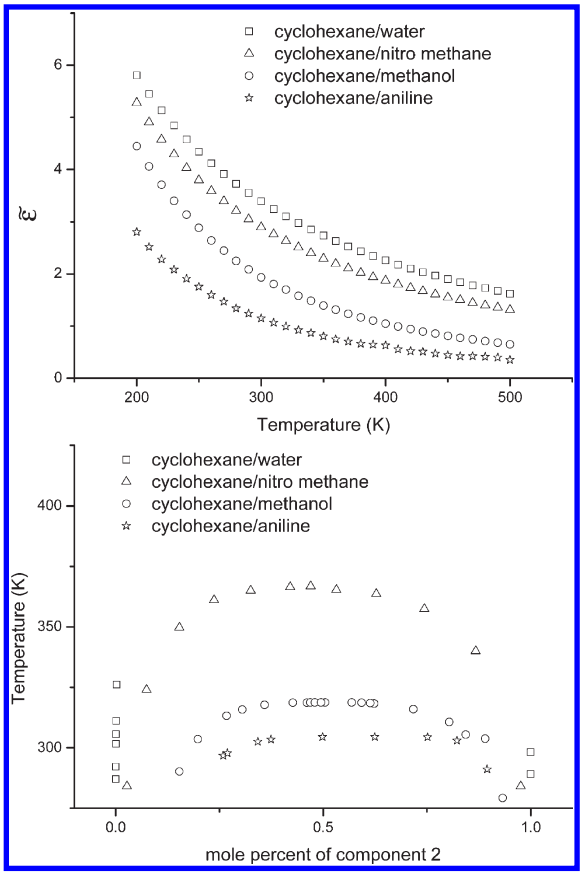

Figure 5. Simulation results and experimental data[30] for cyclohexane mixtures.

$$\frac{\Delta\mu_2}{kT} = \left[\frac{\partial(\Delta A/N_r kT)}{\partial N_2}\right]_{T,V,N_1} \tag{8}$$

A coexistence curve can be determined from the following conditions

$$\Delta\mu_1' = \Delta\mu_1'' \tag{9}$$

$$\Delta\mu_2' = \Delta\mu_2'' \tag{10}$$

where $\Delta\mu_i$ is the change in chemical potential upon isothermally transferring component i from the pure state to the mixture. The primes denote two phases at equilibrium. We require the experimental coordinates of the critical point for phase equilibrium calculation, and the critical condition is given by

$$\frac{\partial(\Delta\mu_1/kT)}{\partial\phi_2} = \frac{\partial^2(\Delta\mu_1/kT)}{\partial{\phi_2}^2} = 0 \tag{11}$$

3.2. Energy Behavior and Miscibility. The degree of miscibility and LLE types depend on energy behavior. The reduced interchange energy $\tilde{\varepsilon}$ is the primary factor that determines the miscibility. In general, the lower the value of $\tilde{\varepsilon}$, the more miscible the mixture and, especially, negative values of $\tilde{\varepsilon}$ lead to full miscibility throughout the whole binary concentration range. To understand whether the system is miscible or immiscible, the critical value of $\tilde{\varepsilon}$ is computed by eq 11. Once the molecular sizes of the mixtures are fixed, eq 11 provides both the critical reduced interchange energy, $\tilde{\varepsilon}_c$, and the critical composition, ϕ_c. If $\tilde{\varepsilon}$ is considerably greater than the critical value, then the mixture is completely separated, and if $\tilde{\varepsilon}$ is slightly greater than the critical value, the mixture is partially miscible, in which the two phases can be present with both of the components in both of the phases.

Figure 1 depicts schematically the temperature dependence of $\tilde{\varepsilon}$, as suggested by the presence of T in the denominator of eq 4. In the system of Figure 1a, if T is lower than T_c, phase separation is induced, and if T is greater than T_c, the system is miscible. Therefore, the energy behavior in Figure 1a produces only an UCST type LLE behavior. On the other hand, the system of Figure 1b can produce all three types of LLE (UCST, LCST, closed-loop miscibility) according to the experimental range. If the experimental range is from T_1 to T_2, only LCST is observed, if from T_2 to T_3, only UCST is seen, and if from T_1 to T_3, closed-loop miscibility behavior is observed. All of the simulation results in this study are divided into these two types of energy behavior. In this work, the energy behavior in Figure 1a is defined as type A, and that in Figure 1b as type B.

4. RESULTS AND DISCUSSION

4.1. LCST and Closed-Loop Miscibility. There are some limitations on the simulation accuracy in this type of calculation. For example, the calculated results are strongly dependent on the force field so the calculated results may differ greatly if the other force field is applied. In addition, the model calculation is

dx.doi.org/10.1021/jp2001628 |J. Phys. Chem. B 2011, 115, 6051–6060

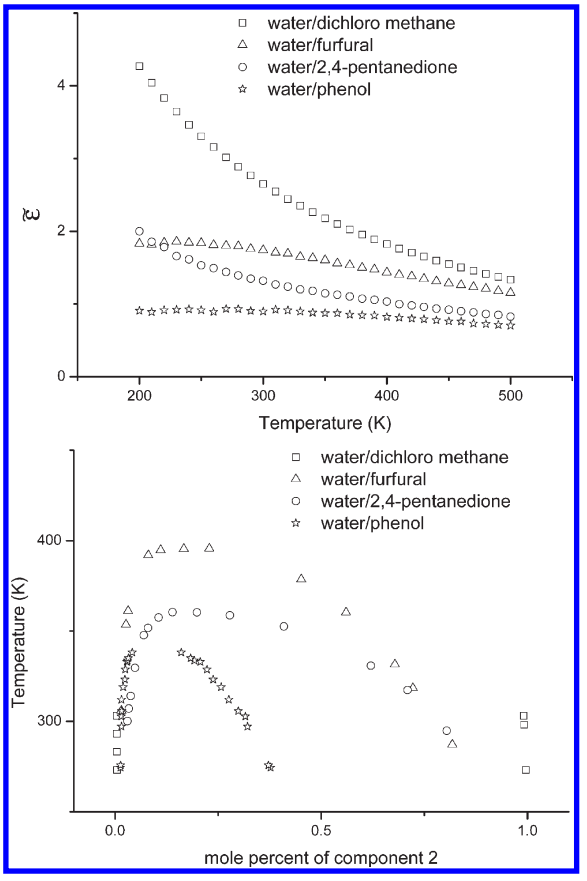

Figure 6. Simulation results and experimental data[30] for water mixtures.

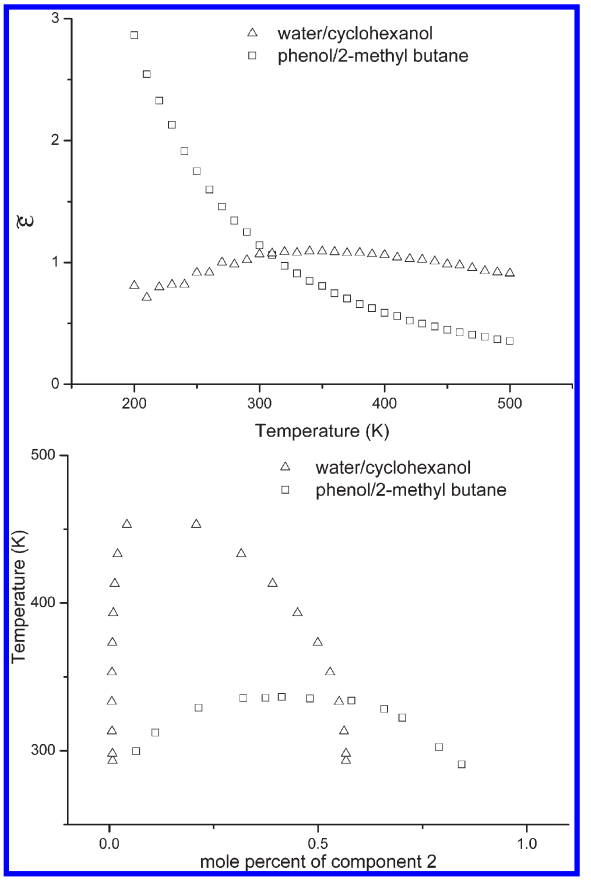

Figure 7. Simulation results and experimental data[30] for water/cyclohexanol and phenol/2-methylbutane.

sensitive to the computational precision and thus the prediction of the energy parameter with great accuracy is very difficult. Being aware of the limitations of simulation accuracy, the present section provides relative comparisons in a qualitative way. In accordance with section 3.2, we first investigated the cause of the LCST (including closed-loop miscibility). This phase behavior may be due to highly oriented interactions in small molecule systems. The oriented interactions are energetically favorable, but entropically unfavorable because of their highly directional-specific characters upon pair formation. Therefore, in the presence of specific interactions between dissimilar components, the mixture formed a homogeneous stable phase. In numerous thermodynamic studies,[9,32,34−36] additional parameters are introduced to take specific interactions into account, and then values are obtained in light of the experimental observations. However, this traditional method is limited and does not serve as a predictive tool because the systems containing the specific interactions do not always induce the LCST. As a matter of fact, although the system contains possible factors of specific interactions, most of them have the UCST.

The method presented here was able to predict the LLE types without any additional concepts. Figure 2a shows the simulation results of water/nitrogen compounds. Water systems with nitroethane and pentanedioic acid, dinitrile result in type A energy behavior so that we expect only UCST LLE behavior. The experimental data are consistent with these results. Water systems with dipropylamine and 1-azacycloheptane indicate the type B energy behavior, and the experimental data show the LCST in dipropylamine, and closed-loop miscibility in 1-azacycloheptane.

Table 1. Systems Investigated in Correlation Studies

Systems	(1)	(2)
A	aniline	hexane
B	glycerol	acetophenone
C	phenol	octane
D	2,2,4-trimethylpentane	perfluorotributylamine
E	water	dichloromethane
F	water	3-methylpyridine
G	water	pentanedioic acid, dinitrile
H	water	nicotine

Similar studies of the water/oxygen compounds are also shown in Figure 2b. Water systems with 2-butoxyethanol and 1-propoxy-2-propanol have a range of increasing $\tilde{\varepsilon}$ obviously, and closed-loop miscibility is reported from experimental observations. The simulation results of glycerol mixtures are also shown in Figure 2c. Glycerol systems with benzaldehyde and acetophenone, which represent UCST experimentally, show the type A energy behavior, and the glycerol/benzyl ethyl amine systems, which have closed-loop miscibility, show the type B energy behavior. Reasonable agreement between the simulation results and experimental data confirms the successful application of the method to real systems. The proposed method accurately provides neither the critical temperature nor the immiscibility region, but it brings insight into what leads to these unusual phenomena.

dx.doi.org/10.1021/jp2001628 |J. Phys. Chem. B 2011, 115, 6051–6060

4.2. Degree of Miscibility. The influence on the degree of miscibility of any given component can be examined by comparing the simulation results for each component while fixing one component of the binary. Figure 3 shows both the simulation results and the experimental temperature−composition data for carbon disulfide mixtures. As discussed above, the higher the value of $\tilde{\varepsilon}$, the less miscible the mixture is. As it can be seen, the highest energy of the carbon disulfide/water system induces the most immiscible region in the corresponding temperature ranges, and as the carbon disulfide system in nitro methane has a higher energy value than in methanol so the carbon disulfide/nitromethane has a higher critical temperature. Similar comparison studies of degree of miscibility are also shown in Figures 4−6 for hexane, cyclohexane, and water mixtures and all of the simulation results agree well with experimentally observed miscibility.

In some cases, the immiscible region decreased steeply near a critical region; in other cases, it decreased gradually. The classical lattice theories, which do not take into account the temperature dependence of the energy parameter, are not able to explain such behavior. We can examine this dependence of miscibility variation on temperature using the simulation results. For example, as can be seen in Figure 6, the experimentally observed two-phase region of the water/2,4-pentanedione system decreased more steeply than the water/furfural system as the temperature increased. Both systems exhibited comparable amounts of miscibility at low temperatures, but the critical temperatures of the two were quite different. The corresponding simulation results also show similar energy values at low temperatures, but the differences in the energy values between the two increased as temperature increased. This can be explained more clearly by the results in Figure 7. The water/cyclohexanol system was more miscible than the phenol/2-methylbutane system near a temperature of 300 K, but the situation was reversed at about 330 K and the critical temperature of the water/cyclohexanol

Table 2. r_2, κ, and $\tilde{\varepsilon}$ Functions of the Systems Investigated in Correlation Studies

			eq 13			
systems	r_2	κ	$10^{-1}a$	$10^{2}b$	$10^{5}c$	$10^{7}d$
A	1.28		−0.675	−0.214	1.05	
B	1.34		−3.89	4.55	0.621	
C	1.65	0.12	2.16	−2.51	14.6	
D	2.23	0.18	7.53	−7.60	2.54	
E	2.92	0.3	−6.98	10.3	−0.0610	
F	4.95	0.39	−15.8	21.8	−5.86	4.36
G	5.25	0.59	1.84	0.249	1.15	
H	5.98	0.53	26.4	35.3	−10.0	8.20

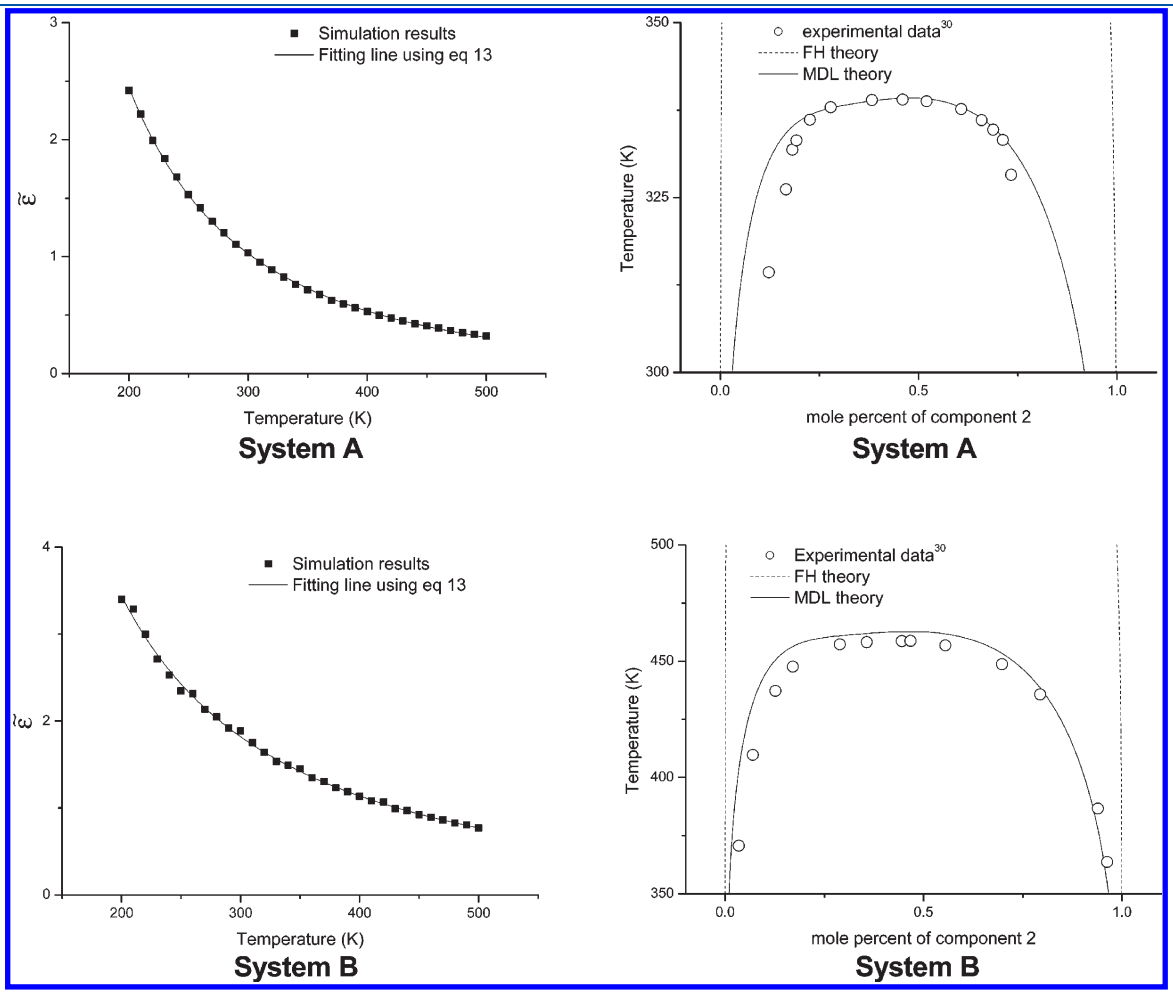

Figure 8. Simulation results and calculated phase diagrams for systems A and B.

dx.doi.org/10.1021/jp2001628 |J. Phys. Chem. B 2011, 115, 6051–6060

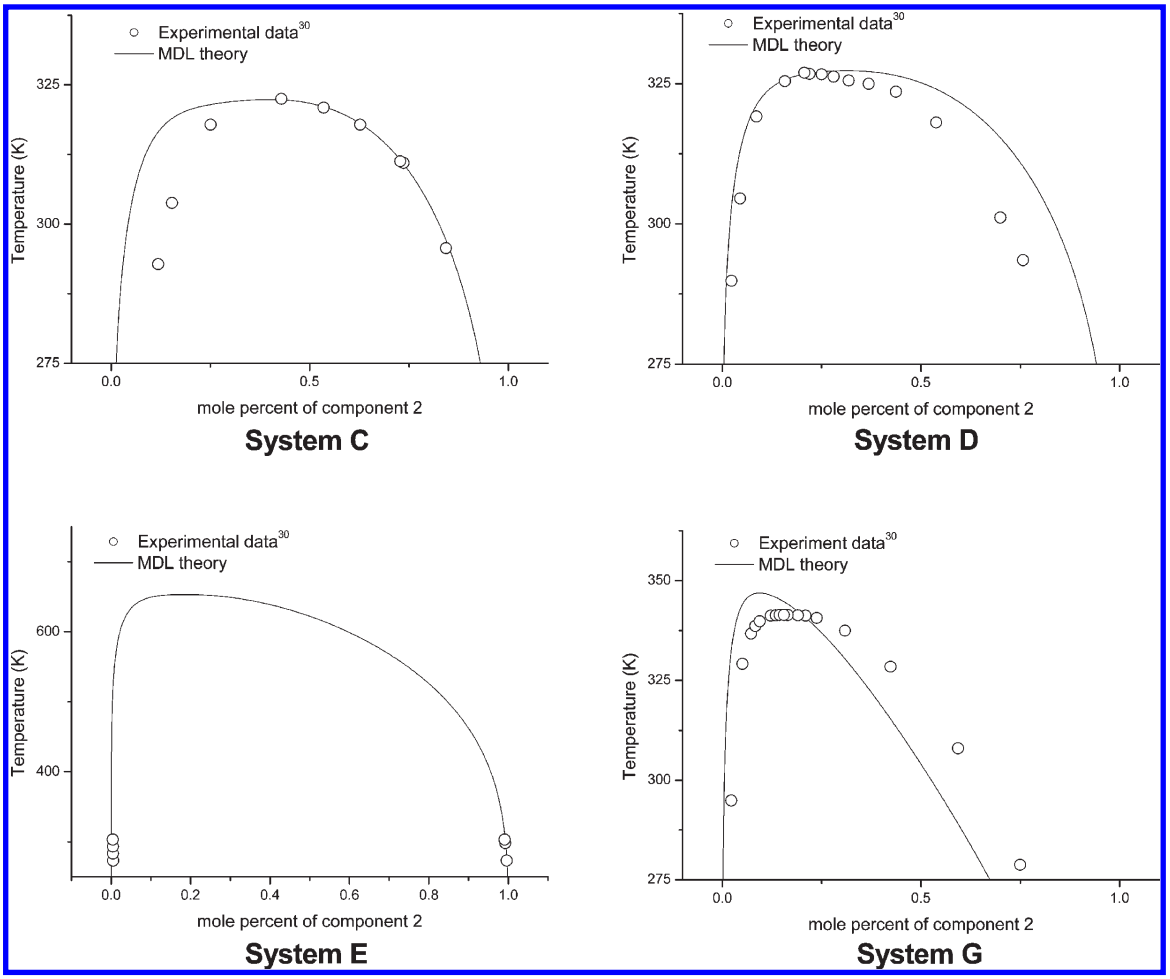

Figure 9. Calculated phase diagrams for systems C, D, E, and G.

system was about 130 K higher than that of the phenol/2-methylbutane system. The simulation results reflect both energy shifts at about 330 K and the differences in miscibility trends between them.

4.3. Thermodynamic Modeling. In this section, thermodynamic modeling and the correlation method are presented to describe temperature−composition diagrams. MDL theory was applied to calculate coexistence curves, and energy parameters obtained from simulation results were directly used in modeling. We defined the smaller molecule as component 1 and the other molecule as component 2. The molecular size parameters are given by the classical method

$$r_2 = \frac{V_{w,2}}{V_{w,1}} \tag{12}$$

where $V_{w,1}$ and $V_{w,2}$ are van der Waals volumes given by Bondi[37] for the components 1 and 2, and $r_1 = 1$ for the smaller molecule. For convenience of the LLE calculation we fitted $\tilde{\varepsilon}$ versus temperature of this system with the following functional form:

$$\tilde{\varepsilon} = a + \frac{b}{T} + \frac{c}{T^2} + \frac{d}{T^3} \tag{13}$$

Table 1 lists the systems investigated in this calculation, and Table 2 lists r_2 and the $\tilde{\varepsilon}$ function.

The main difficulty involved when linking simulation results and model calculations is related to the size of a lattice site. No two molecules have exactly the same van der Waals volumes or surface areas. Therefore, if the size difference of the two components is small ($r_2 \approx 1$), $\tilde{\varepsilon}$ can be directly used in the model calculation, but if the difference is large ($r_2 > 1$), $\tilde{\varepsilon}$ obtained from simulation results will overestimate the model definition and therefore a scale down is necessary.

Figure 8 presents both the simulation results and the calculated phase diagrams of the two systems, which have similar size components. Comparisons were made between the experimental data and with the predictions obtained from the FH and MDL theories. Some studies suggest that the FH model overestimates the critical temperature,[9,10] and this trend is also evident in this calculation. The MDL model provides more satisfactory predictions than those given by the FH model but slightly overestimates the separation region due to the above-mentioned size mismatch.

A scale down method is needed inevitably to correlate phase diagrams of systems with large size differences. $\tilde{\varepsilon}$ can be reformulated simply as $\tilde{\varepsilon}(1-\kappa)$, where κ reflects the size difference between the two molecules as obtained from the experimental data and we expect that κ increases as r_2 increases. Figure 9 shows the calculation results of the MDL with the use of κ for the five systems, all of which exhibit UCST behaviors. The corresponding simulation results are indicated by the form of eq 12 in Table 2 instead of shown in the figure, and κ is also provided in Table 2. The calculated coexistence

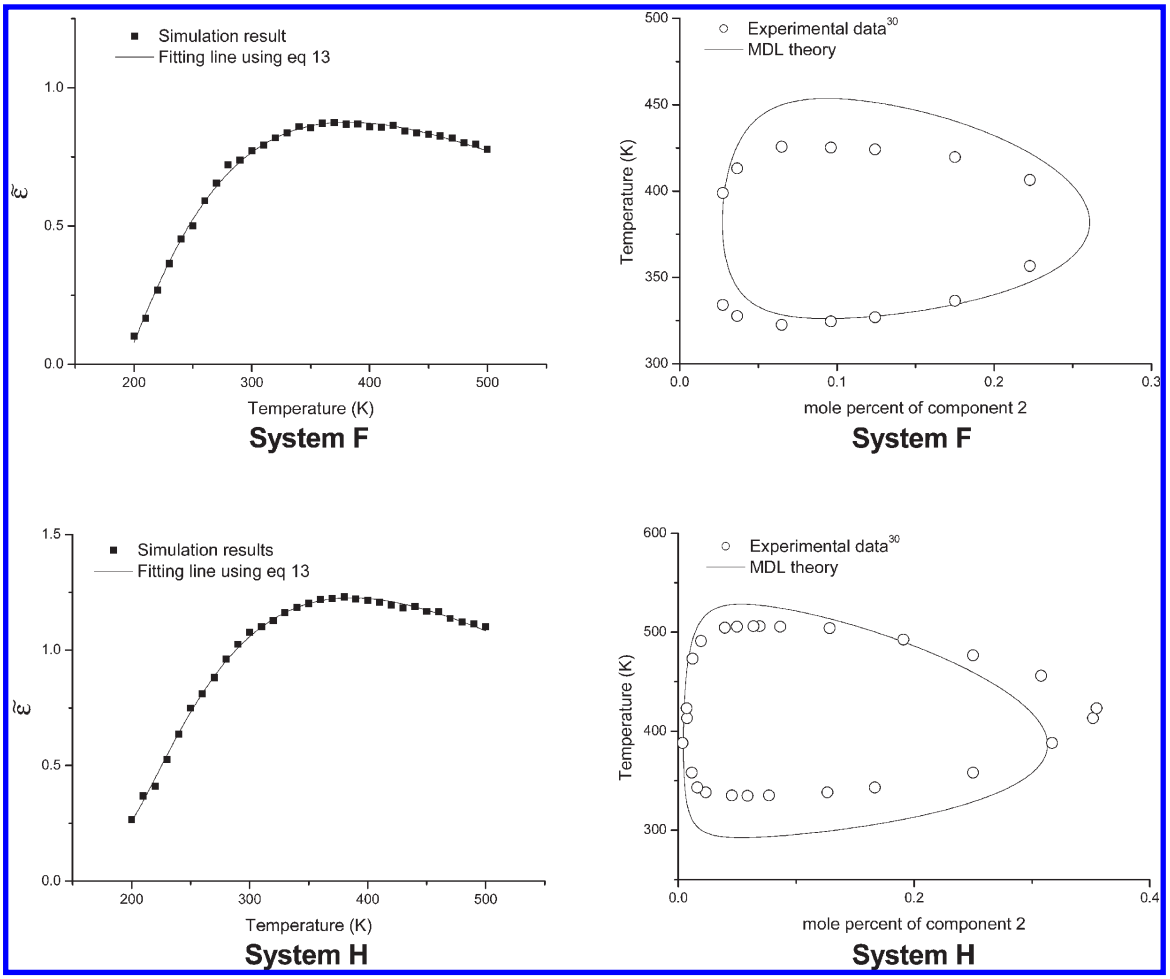

Figure 10. Simulation results and calculated phase diagrams for systems F and H.

curves are well correlated with critical temperature, but not with composition. This is because the predicted r_2 is not precise, and the composition dependence of $\tilde{\varepsilon}$ is not considered in this work. The value of κ increased as r_2 increased, as expected.

According to the results in Figure 9, the method presented here may not be any more appealing than traditional methods, in which the energy parameter is determined by fitting a model to experimental data. The usefulness of the proposed method is seen in the results of the systems shown in Figure 10. These systems, which display a closed-loop immiscibility region (water/3-methylpyridine and water/nicotine), were calculated by the proposed method. The simulation results are also included in Figure 10, and Table 2 provides other information for this calculation. Only one correlating parameter κ was used in this calculation, which is the same way as a case of UCST. Although the results are not finely accurate, the calculated results agree quite well with immiscible temperature ranges. As discussed in section 4.1, traditional methods of correlating closed-loop miscibility introduced additional concepts and parameters to calculate such unusual behaviors. Two or three fitting parameters are used for the calculation of energy parameters,[9,32,34−36,38,39] and the obtained values are arbitrary set to fit the temperature dependence of the energy parameter. The method presented here is more physically acceptable because these additional parameters are not used in the calculations.

Assuming that the simulated energy values increase linearly with size differences, it might be better interpreted by using the functional form of κ, after fitting, yielding the following equation:

$$\kappa = 0.12(r_2 - 1) \tag{14}$$

As depicted in Figure 11, the obtained values of κ converged into eq 14. It is possible to use the proposed method as a predictive tool when using a scaling function such as eq 14. However, it is very difficult to accurately predict the phase diagram because many obstacles are included in this type of calculation.

The problems related to this research are 2-fold; one is related to the molecular simulations and the other to the thermodynamic model. In molecular simulations, finding an appropriate force field for the given systems is important because the calculated results are strongly dependent on the force field that is applied. In this work, we chose the COMPASS force field because other force fields such as Universal[40,41] or Dreiding[42] cannot display the type B energy behavior of some LCST systems. Although COMPASS is suitable for obtaining information about the temperature dependence of energy values in small molecules systems, it does not always correspond well with other chemical systems. An improved approach is to use the dynamics method along with the Amorphous Cell module in the Materials Studio software package, which may provide better results, especially when information about the composition dependence of the energy values is required. However, this procedure is very time-consuming and suitable only for specific

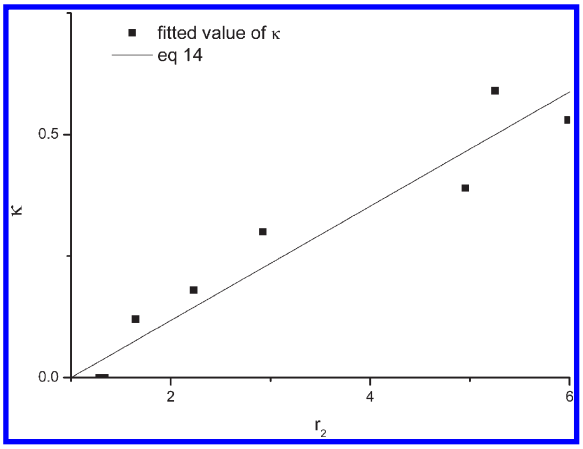

Figure 11. Size dependence of κ.

cases, not for general studies such as the present study, which require large amounts of simulations. In studies of macromolecular systems, additional factors governing miscibility may include molecular weight, chain packing, the degree of crystallinity, and chain flexibility. Although these factors cannot be addressed by atomistic simulations, in this small molecule case, reasonable results were obtained by the Blend module.

There are also limitations in the thermodynamic theory employed for the investigation presented in this paper. The MDL theory gives better results than the FH theory because the MDL theory is based on Monte Carlo simulation results. However, as the size difference of the two components is larger, an additional scaling parameter κ must be used. Although the value of κ can be dealt with according to eq 14, this solution is very restricted; accurate prediction of κ remains elusive. Another problem caused by the size mismatch is that the coordination number z becomes ill-defined. We used a fixed value ($z = 6$) in this work following an assumption of a cubic lattice, but the coordination number varies actually if the two molecules have different size. More specifically, the deviation of the composition dependence is mainly due to an inaccurate value of r_2. In many cases, r_2 is obtained by the fitting method because the r_2 value is hard to define exactly. However, we calculated r_2 simply using the molar volume ratio (eq 12), and thus the calculated curves showed deviations of the critical composition. In addition, lattice models such as the FH model or MDL model do not include variable density, but in real systems density depends on state conditions such as temperature. The experimental data did not perform in a manner consistent with these basic assumptions of the model, resulting in unavoidable deviations.

5. CONCLUSIONS

We performed molecular simulations to calculate pair interaction energies while considering temperature dependence. Comparison studies were implemented using simulation results to predict LLE types and their relative degrees of miscibility in binary liquid mixtures of small molecules. We obtained reasonable agreement with experimental observations. To derive temperature−composition diagrams, thermodynamic models and correlation methods were also presented in conjunction with simulation results. The accuracy of thermodynamic modeling is limited, but the method presented here is widely applicable because it can calculate the model parameters of any chemical system via molecular simulations. There are limitations in the simulations, the thermodynamic model, and the method itself of the proposed approach. Further advancements are required for more accurate prediction of phase miscibility, but this simple procedure can serve as a basis for understanding miscibility problems often encountered in chemical process design.

AUTHOR INFORMATION

Corresponding Author

*E-mail: ycbae@hanyang.ac.kr.

ACKNOWLEDGMENT

This work was supported by Basic Science Research Program through the National Research Foundation of Korea (NRF) grant funded from the Ministry of Education, Science, and Technology (MEST) of Korea for the Center for Next Generation Dye-sensitized Solar Cells (No. 2010-0001842).

REFERENCES

(1) Flory, P. J. *J. Chem. Phys.* **1942**, *10*, 51.
(2) Huggins, M. L. *J. Phys. Chem.* **1942**, *46*, 151.
(3) Guggenheim, E. A. *Mixtures*; Oxford University Press: Oxford, U.K., 1952.
(4) Koningsveld, R.; Kleintjens, L. A. *Macromolecules* **1971**, *4*, 637.
(5) Freed, K. F. *J. Phys. A: Math. Gen.* **1985**, *18*, 871.
(6) Bawendi, M. G.; Freed, K. F.; Mohanty, U. *J. Chem. Phys.* **1988**, *87*, 5534.
(7) Bawendi, M. G.; Freed, K. F. 1988, *88*, 2741.
(8) Dudowicz, J.; Freed, K. F. *Macromolecules* **1991**, *24*, 5076.
(9) Hu, Y.; Lambert, S. M.; Soane, D. S.; Prausnitz, J. M. *Macromolecules* **1991**, *24*, 4356.
(10) Oh, J. S.; Bae, Y. C. *Polymer* **1998**, *39*, 1149.
(11) Schweizer, K. S.; Curro, J. G. *Adv. Polym. Sci.* **1994**, *116*, 321.
(12) Schweizer, K. S.; Curro, J. G. *Adv. Chem. Phys.* **1997**, *98*, 1.
(13) Chen, Y. L.; Schweizer, K. S. *J. Phys. Chem. B* **2004**, *108*, 6687.
(14) Jayaraman, A.; Schweizer, K. S. *Macromolecules* **2008**, *41*, 9430.
(15) Taylor, M. P.; Lipson, J. E. G. *J. Chem. Phys.* **1995**, *102*, 2118.
(16) Luettmer-Strathmann, J.; Lipson, J. E. G. *Macromolecules* **1999**, *32*, 1093.
(17) White, R. P.; Lipson, J. E. G. *Mol. Phys.* **2008**, *106*, 729.
(18) Heine, D.; Wu, D. T.; Curro, J. G.; Grest, G. S. *J. Chem. Phys.* **2003**, *118*, 914.
(19) Jaramillo, E.; Wu, D. T.; Grest, G. S.; Curro, J. G. *J. Chem. Phys.* **2004**, *120*, 19.
(20) Tsige, M.; Curro, J. G.; Grest, G. S. *J. Chem. Phys.* **2008**, *129*, 214901.
(21) McCarty, J.; Lyubimov, I. Y.; Guenza, M. G. *J. Phys. Chem. B* **2009**, *113*, 11876.
(22) McCarty, J.; Lyubimov, I. Y.; Guenza, M. G. *Macromolecules* **2010**, *43*, 3964.
(23) Fan, C. F.; Olafson, B. D.; Blanco, M.; Hsu, S. L. *Macromolecules* **1992**, *25*, 3667.
(24) Patnaik, S. S.; Pachter, R. *Polymer* **2002**, *43*, 415.
(25) Jawalkar, S. S.; Adoor, S. G.; Sairam, M.; Nadagouda, M. N.; Aminabhavi, T. M. *J. Phys. Chem. B* **2005**, *109*, 15611.
(26) de Arenaza, I. M.; Meaurio, E.; Coto, B.; Sarasua, J. R. *Polymer* **2010**, *51*, 4431.
(27) Luo, Z.; Jiang, J. *Polymer* **2010**, *51*, 291.
(28) Sun, H. *J. Phys. Chem. B* **1998**, *102*, 7338.
(29) Sun, H.; Ren, P.; Fried, J. R. *Comput. Theo. Polym. Sci.* **1998**, *8*, 229.
(30) Sorensen, J. M.; Arlt, W. *Liquid-liquid Equilibrium Data Collection*; Dechema: Frankfurt, Germany, 1979.
(31) Blanco, M. *J. Comput. Chem.* **1991**, *12*, 237.
(32) Oh, S. Y.; Bae, Y. C. *Polymer* **2008**, *49*, 4469.
(33) Madden, W. G.; Pesci, A. I.; Freed, K. F. *Macromolecules* **1990**, *23*, 1181.
(34) ten Brinke, G.; Karasz, F. E. *Macromolecules* **1984**, *17*, 815.

(35) Sanchez, I. C.; Balazs, A. C. *Macromolecules* **1989**, *22*, 2325.
(36) Hino, T.; Lambert, S. M.; Soane, D. S.; Prausnitz, J. M. *AIChE. J.* **1993**, *39*, 141.
(37) van Krevelen, D. W. *Properties of Polymers*, 3rd ed.; Elsevier: Amsterdam, 1990.
(38) Qian, C.; Mumby, S. J.; Eichinger, B. E. *Macromolecules* **1991**, *24*, 1655.
(39) Xu, X.; Peng, C.; Cao, G.; Liu, H.; Hu, Y. *Ind. Eng. Chem. Res.* **2009**, *48*, 7828.
(40) Rappé, A. K.; Casewit, C. J.; Colwell, K. S.; Goddard, W. A.; Skiff, W. M. *J. Am. Chem. Soc.* **1992**, *114*, 10024.
(41) Rappé, A. K.; Colwell, K. S.; Casewit, C. J. *Inorg. Chem.* **1993**, *32*, 3438.
(42) Mayo, S. L.; Olafson, B. D.; Goddard, W. A. *J. Phys. Chem.* **1990**, *94*, 8897.